

Self-organization in porous silicon formation

George C. John and Vijay A. Singh

Physics Department, I.I.T., Kanpur, 208106 Uttar Pradesh, India

(Received 4 December 1996)

We investigate the diffusion-induced nucleation model for the formation of porous silicon. We show that simulations based on this model can explain experimental features such as (i) a constant porosity profile, (ii) a planar film front, and (iii) the effect of the surface roughness on the porosity profile. We show that for a critical roughness the surface nanoporous layer disappears. Further, these simulations highlight aspects of self-organization in the pore formation process. [S0163-1829(97)03832-0]

The formation of porous silicon during the anodization of crystalline silicon (*c*-Si) has been extensively studied for the past four decades.^{1,2} Several computer simulations suggest that diffusion-limited phenomena play an important role in the pore formation.³⁻⁵ Porous silicon films of thickness up to 500 μm have been fabricated, which exhibit a constant porosity⁶ and a planar porous film front.^{7,8}

The recent spurt of interest in porous silicon has been sparked by the observation of visible photoluminescence from high porosity samples⁹ (porosity $\rho \geq 60\%$). The earlier diffusion limited models were not successful in obtaining high porosity structures. This limitation was overcome by the diffusion-induced nucleation (DIN) model.⁵ The aim of this work is to highlight aspects of self-organization during pore formation process and explain experimental features such as (i) a constant porosity profile,⁶ (ii) a planar film front,^{7,8} and (iii) the effect of the surface roughness on the porosity profile.^{8,10}

The DIN model for porous silicon formation employs three parameters, namely (i) a depletion layer width ΔW , (ii) a drift length " l " which governs ballistic transport, and (iii) a nucleation probability $(1-p_t)$ with which a pore can propagate at random to nearest neighbors. Note that p_t is the termination probability where $p_t \in [0,1]$. ΔW and l are two antithetical scales, one separating the particle from the aggregate, the other driving it towards the aggregate. Tuning the relative values of ΔW and l produces a variety of morphologies.¹¹ In this work we shall explore the effect of the nucleation process $(1-p_t)$ mainly in the diffusion dominated limit ($\Delta W > l$) of the DIN model.

There is no consensus on the exact definition of self-organized criticality¹² (SOC). Nonequilibrium macroscopic systems deemed to exhibit SOC are characterized by microscopic short-range interactions which occur as extremely fast responses to the external driving field, resulting in scale-invariant behavior. Self-organized criticality has been observed in various computer models of sandpiles, forest fires, and earthquakes.¹³ In this context, we examine the formation of porous silicon which exhibits a uniform density of pores beyond an initial surface region. This constant porosity profile is seen in porous silicon films of widely differing porosities.⁶ The DIN model for formation assumes the presence of a macroscopic diffusion process which triggers a short-range nucleation process. We shall examine the effect

of this nucleation process on the porosity profile and show that the model exhibits signatures of self-organized criticality.

We observe that our simulations yield a pore front which propagates uniformly in consonance with experimental studies. One obtains a plateau of constant porosity and observes that at the pore (film) front the porosity falls sharply to zero. The plateau and the sharpness of the film front are studied as a function of the pore nucleation probability $(1-p_t)$ in our model. The fall in porosity at the film front is seen to be sharper with decreasing p_t .

We then show that in the limit when the time scales associated with the nucleation process are made infinitesimally small, the system stabilizes to a constant critical porosity structure over distances of the order of the lattice size. This critical porosity is seen to be determined solely by the control parameters of the macroscopic diffusion field $\{\Delta W, l\}$. This is indicative of self-organization in porous silicon formation.

We further carry out studies on the effect of the substrate roughness on pore morphologies and compare them with experimental results. We also explain the experimentally observed marginal decrease in porosity with increasing substrate roughness.¹⁰

Before we proceed to experiment with the parameters of the simulation, let us briefly recapitulate the DIN model⁵ for the sake of completeness. The steps in the simulation are as follows: (i) The simulation is carried out on a rectangular lattice, one side of which represents the linear substrate. For the case of porous silicon this is the HF-Si interface. Periodic boundary conditions are imposed in the lateral direction. (ii) Aggregation (dissolution in the case of porous silicon) occurs when a particle (a hole in the case of silicon) diffuses from the interior (the bulk) to the linear substrate. Initially, no particles are present within a distance ΔW from the linear substrate. ΔW defines a depletion layer width. (iii) The particle performs off-lattice random walks until it approaches a distance l of the aggregate. (iv) As soon as the particle comes within a distance l of the aggregate, it is driven to the surface of the aggregate and becomes a part of it. (v) Next, one of the nearest neighbor sites of the newly occupied site is now occupied with probability $(1-p_t)$. This is the propagation process. The termination probability $p_t \in [0,1]$. This represents an etching away of the nearest neighbor site for the case of porous silicon. The depletion layer boundary is

modified to follow the new aggregate contour. (vi) Step (v) is repeated until the occupation of nearest neighbor sites is terminated with probability p_t . Thus the propagation process leads to a *nucleation chain*. (vii) A particle is launched from the interior of the lattice and beyond the depletion layer boundary defined by ΔW . Steps 3 to 6 are repeated. An aggregate (porous structure in the case of porous silicon) is thus formed.

The time scale of the simulation is defined as follows: Each step of the random walk is defined to be one time unit. Once nucleation starts, a single nucleation chain is assumed to take one unit of time. In order to examine the effect of the nucleation process, we vary the probability p_t , keeping the control parameters $\{\Delta W, l\}$ constant. This corresponds to changing the time scale of the nucleation at a single site. This is easily understood as follows. We consider the mean size $\langle l \rangle$ of the *nucleation chain* as the average number of sites dissolved. This is given by

$$\langle l \rangle = \frac{1}{p_t}.$$

Since this aggregation (dissolution for porous silicon) of the whole chain occurs in unit time, the average time associated with a single site occupation (dissolution) is

$$\tau_d \approx \frac{1}{\langle l \rangle} = p_t.$$

As p_t goes to zero there is an infinite separation between the microscopic nucleation process and the macroscopic diffusion process.

We now present the results based on our model. The simulations are carried out on a 250×800 lattice with the shorter side representing the interface. The plots presented have been typically averaged over five runs with varying initial conditions of the random number generator. We have ensured that the results presented are robust by going to larger lattice sizes and averaging over a larger number of runs.

Figure 1 represents the porosity $\rho(Z)$ versus depth Z obtained for $\Delta W=8$, $l=2$ for various termination probabilities. Note that $\Delta W > l$ and this as discussed in an earlier work¹¹ represents the diffusion-limited regime. The inset depicts a typical porosity profile obtained in the DIN model. This plot can be divided into three regions: (i) An initial zone ΔZ_i of high porosity with a possible fractal character (shaded region). This zone has been termed ‘‘nanoporous’’ in the porous silicon experimental literature.⁶ (ii) A zone ΔZ_c of constant porosity ρ_c . This plateau region has been termed as ‘‘macroporous.’’ (iii) A growth zone ΔZ_g representing the film front. Here $\Delta Z_i + \Delta Z_c + \Delta Z_g = Z_d$ represents the total depth of the porous silicon layer. In the case of porous silicon it has been experimentally observed that the porosity ρ remains approximately constant with the depth beyond a thin surface region (ΔZ_i of Fig. 1). This has been successfully reproduced by our model. A straightforward diffusion-limited aggregation implementation ($\Delta W > l$ and $p_t = 1.0$) would yield a monotonically decreasing porosity profile¹⁴ [$\rho(Z) \approx Z^{-1/3}$]. Note that the constant porosity plateau region ΔZ_c is obtained only if there is a finite probability for pore propagation, i.e., $p_t < 1$.

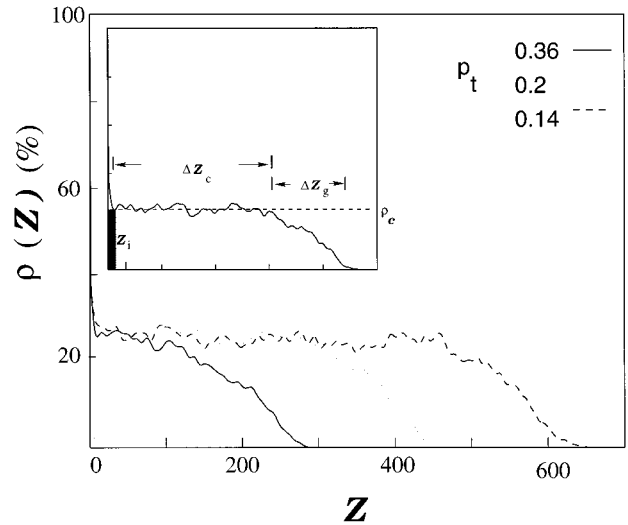


FIG. 1. Porosity profiles in the diffusion regime $\Delta W > l$. The inset shows a typical porosity profile in the diffusion regime $\Delta W > l$, which can be divided into three regions: (i) An initial zone ΔZ_i , indicated by the shaded region, of high porosity. (ii) A zone ΔZ_c of constant porosity ρ_c . (iii) A growth zone ΔZ_g representing the film front. The graph depicts porosity profiles for different values of p_t . As the termination probability p_t is lowered the width of the plateau region ΔZ_c increases with little change in the plateau porosity ρ_c . The depth Z is expressed in lattice units.

As discussed in the previous paragraph a value of $p_t < 1$ is necessary to obtain the plateau region. However the value of the mean porosity ρ_c in the plateau region is otherwise independent of p_t . This is illustrated in Fig. 1 where we plot the porosity profiles obtained with $\Delta W=8$, $l=2$, and p_t varying from 0.36 to 0.14. The number of random walkers was kept fixed in these simulations. Figure 1 indicates that as p_t is decreased: (i) the initial interface zone ΔZ_i remains constant, (ii) the plateau zone ΔZ_c increases in length, (iii) the plateau porosity remains constant, and (iv) the growth zone ΔZ_g representing the film front decreases. The termination probability p_t simply serves to define the extent of the plateau region ΔZ_c . The fact that ρ_c does not depend on p_t maybe understood as follows. The diffusion-limited process has a higher probability of picking out the tips of the growing aggregate for further nucleation. Lateral dissolution (nucleation) can effectively eliminate further diffusion into the porous structure on account of the presence of the drift length l . This is similar to the ‘‘pinch off’’ effect in the phenomenological Beale model.⁷ We have also examined the density-density correlation function $C(Z)$.¹⁴ Like the porosity profiles of Fig. 1 it is constant in the plateau region. Thus the correlation length $\xi \approx \Delta Z_c$, i.e., the extent of the plateau zone. We have confirmed this by performing calculations for larger lattice sizes.

We next examine the dependence of the correlation length ξ on the termination probability p_t , and consequently the time scale associated with the short-range nucleation process. In Fig. 2 we plot ξ versus p_t on a log-log scale (solid line, empty boxes). They are seen to be related by the power law

$$\xi \propto p_t^{-\beta}. \quad (1)$$

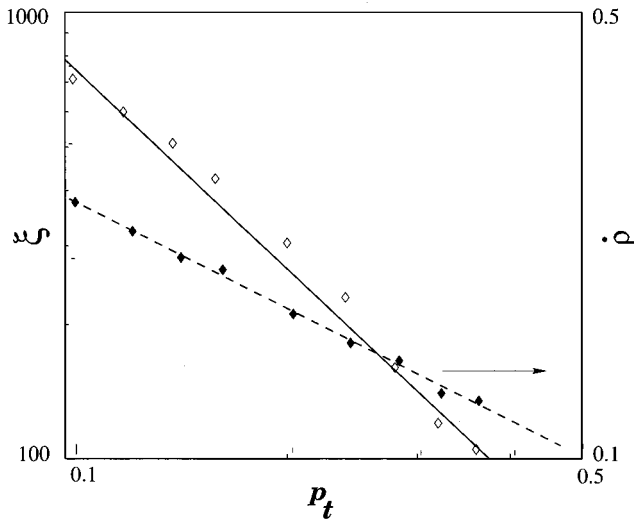


FIG. 2. Dependence of the correlation length ξ on the termination probability p_t (solid line, empty boxes). This length which is also a measure of the plateau zone ΔZ_c of Fig. 1 is seen to diverge for small p_t with an exponent of ≈ 1.5 . The broken line (filled boxes) depicts the dependence of the rate of fall of the porosity in the growth zone ΔZ_g ($\dot{\rho}$, right hand y axis) on the termination probability p_t . This rate diverges for small p_t with an exponent 0.6 (± 0.1). Note that the plots are on a log scale. ξ is expressed in lattice units.

Here the exponent β depends on ΔW and l [$\beta = \beta(\Delta W, l)$]. In the diffusion-limited regime ($\Delta W \gg l$), we find that $\beta = 1.5(\pm 0.1)$. Hence the correlation length diverges as $p_t \rightarrow 0$ in a power law fashion. In porous silicon one finds a constant porosity layer⁸ of thicknesses as large as $500 \mu\text{m}$. Further it is experimentally observed that the film front is sharp. In other words the zone ΔZ_g of Fig. 1 is narrow. A simple nucleation process in the absence of diffusion resembles “Eden” modellike growth and is expected to give a planar film front. Therefore as p_t is decreased, diffusion effects become less dominant and we can expect the film front to become sharper. It would be useful to examine the rate of fall in the porosity in the growth region,

$$\dot{\rho} = \frac{\rho_c}{\Delta Z_g},$$

where ρ_c is the plateau porosity. Figure 2 also depicts a plot of $\dot{\rho}$ with p_t (broken line, filled boxes). It is observed that

$$\dot{\rho} \sim p_t^{-\gamma}. \quad (2)$$

The exponent γ depends on ΔW and l [$\gamma = \gamma(\Delta W, l)$]. In the diffusion-limited regime discussed in this work ($\Delta W > l$), we find that $\gamma = 0.6(\pm 0.1)$. This suggests that $\Delta Z_g \rightarrow 0$ as $p_t \rightarrow 0$.

We now examine the effect of substrate roughness on the self-organized state. Roughening is implemented as follows: (i) Start with the first site on the linear interface. (ii) Choose a random integer $r \in [0, Z_r]$ with uniform probability. Here Z_r is a roughness parameter. (iii) Create a trench of depth r , i.e., etch away r sites starting from the interface. (iv) Move to the next interface site, repeat (ii) and (iii).

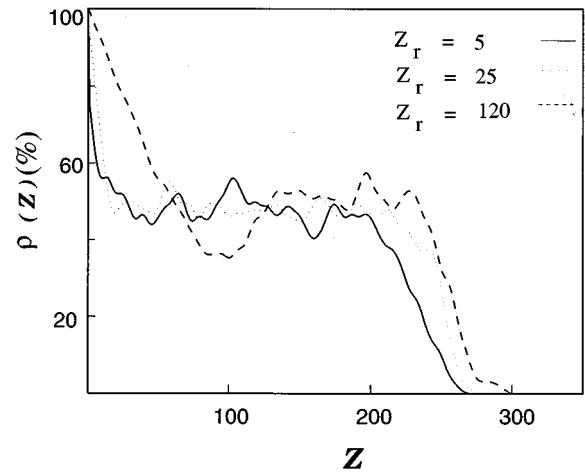


FIG. 3. Porosity profiles for three different values of the roughness parameter. We are interested in the interface region and hence the depth ranges up to 350 lattice units in the figure. The simulations were run on much larger lattices of size 250×800 . The depth Z is expressed in lattice units.

Roughening results in a linear porosity profile in the region $0 \leq Z \leq Z_r$. The depletion layer boundary is then suitably modified to follow the new interface contour at a distance ΔW . The resulting porosity profiles in such simulations with varying values of Z_r are depicted in Fig. 3. The numerical values of the other parameters are $\Delta W = 3$, $l = 5$, and $p_t = 0.4$. The initial rough surface is seen to retain a linear porosity profile even after the etching process. This is indicative of the lack of penetration of the diffusing particle into the initial roughened zone. We also see that for a critical roughness, the “nanoporous” Si layer ΔZ_i disappears. This happens when the initial rough zone has a porosity value close to ρ_c . On increasing the roughness further (i.e., increasing Z_r), a macroporous layer is formed at the top, with porosities less than ρ_c . This is indicated by the porosity profile $Z_r = 120$ in Fig. 3.

There exists experimental confirmation of this result by Lehmann⁸ who hypothesizes a critical current density where all charge transfer takes place through the pore tips. Experimentally, it has been possible to etch a pattern on the substrate, which can be made to grow linearly inward, for specific values of the anodization current and electrolyte concentration. The critical porosity established on the surface is thus maintained constant into the bulk in a manner similar to our simulation.

Another experimental study due to DiFrancia¹⁰ demonstrates that the mean porosity of the porous silicon layers decreases marginally with the interface roughness. Our results can be used to explain the observation. DiFrancia defines the mean porosity $\bar{\rho}$ to be

$$\bar{\rho} = \frac{\text{Mass of Si wafer} - \text{Mass of PS film}}{\text{Mass of Si Wafer}},$$

assuming complete conversion of Si to porous silicon (PS). The experimental study was carried out with samples of thicknesses $12\text{--}15 \mu\text{m}$ with trench depths up to $0.7 \mu\text{m}$. Our simulations show that the mean porosity of the initial “nan-

oporous" zone decreases constantly with increasing roughness. This is manifested as a small decrease in the mean porosity of the entire PS sample.

The DIN model simulates a nonequilibrium, nonconserving dissolution process. In the diffusion-limited regime ($\Delta W > l$) it produces a statistical steady state of constant porosity. In earlier studies of diffusion-limited deposition onto a linear substrate¹⁴ a porosity profile of the form $\rho(Z) \sim Z^{-k}$ has been obtained where $k \approx 0.3$. In the DIN model discussed here, this corresponds to $\Delta W \gg l$ and $p_t = 1.0$. We have shown that the introduction of a short-range nucleation process, controlled by the termination probability $p_t < 1.0$ yields a statistical steady state exhibiting constant porosity. The limit $p_t \rightarrow 0$ corresponds to an infinite separation of time scales and leads to a constant porosity plateau of the size of the lattice. No further fine tuning of the parameters or long-range diffusion process is required to ensure this. This type of behavior is commonly encountered in models of self-organized criticality.¹²

The DIN model however differs from conventional models of SOC in certain respects. For instance, this algorithm does not employ a global updating step, as in the sandpile or forest fire models. Once the site is etched, it remains etched and there is no further need for relaxation or regeneration. The self-organization is achieved by the short-range nucleation process, rather than an "avalanche" of events. However, the presence of power law behavior as evinced in Eqs. (1) and (2) suggests the presence of a critical state.

Another difference between the porous silicon system and the various SOC models in literature is the presence of an external diffusive driving field. In sandpiles, forest fires, or word processors,¹⁵ an "avalanche" can be triggered from any site at random. In the case of the DIN model, the probability of the short-range nucleation process occurring at the tip sites is much larger because of the diffusive nature of the external field. The self-organized state is possible because at

some stage, there is a complete cutoff of the diffusing particles into the structure beyond the growth zone.

In studying the nature of the self-organized state, we have considered the case $\Delta W > l$. For the complementary situation $l < \Delta W$, the ballistic process dominates the diffusive field. Ballistic processes are known to produce constant density profiles,¹⁶ and hence in this case a short-range process is not needed to obtain the observed density profile. Varying p_t in these simulations will lead to differing values of the plateau porosity ρ_c . Note that the roughness studies carried out with $\Delta W < l$ (Fig. 3), yield similar results even in the case of $\Delta W > l$.

Some workers have hypothesized that silicon nanocrystallites of diameters $\approx 15 \text{ \AA}$ are responsible for the visible luminescence of porous silicon.¹⁷ Such small crystallites are likely to be found in the surface "nanoporous" layer ($Z \leq \Delta Z_i$ of Fig. 1). Our results indicate that the "nanoporous" layer is strongly dependent on the initial substrate roughness (see Fig. 3). Consequently one would expect the photoluminescence in porous silicon to be affected by the substrate roughness. We suggest that experiments along these lines be conducted.

We have presented a result where the introduction of a short-range nucleation process into a diffusion-limited system results in a self-organized state. The pore density in the self-organized state is independent of the nucleation process as well as initial conditions such as the substrate roughness. This model is used to explain experimental features such as (i) a constant porosity profile, (ii) a planar film front, and (iii) the effect of the surface roughness on the porosity profile. We have predicted that for a critical value of the substrate roughness, the initial nanoporous layer will disappear.

We would like to acknowledge support from the Council of Scientific and Industrial Research, Government of India and the Department of Science and Technology, Government of India.

¹R. L. Smith and S. D. Collins, J. Appl. Phys. **71**, R1 (1992).

²G. C. John and V. A. Singh, Phys. Rep. **263**, 93 (1995).

³R. L. Smith, S.-F. Chuang, and S. D. Collins, J. Electron. Mater. **17**, 533 (1988).

⁴J. Erlebacher, K. Sieradzki, and P. C. Searson, J. Appl. Phys. **76**, 182 (1994).

⁵G. C. John and V. A. Singh, Phys. Rev. B **52**, 11 125 (1995).

⁶N. Ookubo, J. Appl. Phys. **74**, 6375 (1993).

⁷M. I. J. Beale *et al.*, J. Cryst. Growth **73**, 622 (1985).

⁸V. Lehmann, J. Electrochem. Soc. **140**, 2836 (1993).

⁹L. T. Canham, Appl. Phys. Lett. **57**, 1046 (1990).

¹⁰G. DiFrancia, Solid State Commun. **87**, 451 (1993).

¹¹G. C. John and V. A. Singh, Phys. Rev. E **53**, 3920 (1996).

¹²G. Grinstein and C. Jayprakash, Comput. Phys. **9**, 164 (1995).

¹³P. Bak, C. Tang, and K. Wiesenfeld, Phys. Rev. A **38**, 364 (1988).

¹⁴P. Meakin, Phys. Rev. B **30**, 4207 (1984).

¹⁵W. Bauer and S. Pratt, Phys. Rev. E **54**, R1 009 (1996).

¹⁶P. Meakin, Phys. Rev. A **27**, 2616 (1983).

¹⁷S. Schuppler *et al.*, Phys. Rev. B **52**, 4910 (1995).